Ultrathin organic transistors for chemical sensing

Richard D. Yang, T. Gredig, Corneliu N. Colesniuc, Jeongwon Park, Ivan K. Schuller, William C. Trogler, and Andrew C. Kummel[a)]
Integrated Nanosensor Lab, Materials Science and Engineering, Department of Physics and Department of Chemistry and Biochemistry, University of California, San Diego, La Jolla, California 92093

(Received 21 February 2007; accepted 22 May 2007; published online 26 June 2007)

Ultrathin cobalt phthalocyanine transistors of 4 ML have been fabricated for chemical sensing. Compared to 50 ML devices, the ultrathin transistors show faster response times, higher base line stabilities, and sensitivity enhancements of 1.5–20 for the five analytes tested. The enhanced response for the ultrathin transistors provides insight into the device physics. The absorption of analytes changes the surface doping level and trap energies. The changes in surface trap energies perturb the charge transport properties of the ultrathin devices, thereby, making these devices more sensitive. © *2007 American Institute of Physics*. [DOI: 10.1063/1.2749092]

Organic thin-film transistors (OTFTs) are candidates for chemical vapor sensing due to a strong charge transport dependence on the chemical environments.[1–6] Herein, OTFTs employed for chemical sensing using small organic materials are denoted as chemically sensitive field-effect transistors (ChemFETs). Previous studies on ChemFETs used relatively thick films (>10 ML).[1–7] In this work, cobalt phthalocyanine (CoPc) films as thin as 4 ML have been deposited by organic molecular beam epitaxy (OMBE). In the absence of analytes, these devices show mobilities comparable (within a factor of 3) with films as thick as 50 ML. However, we have demonstrated significant improvements in the chemical response, base line stability, and sensing kinetics using the ultrathin ChemFETs. The differences in chemical response and kinetics between the ultrathin and thick ChemFETs provide insights into the sensing physics of the ChemFETs.

Fundamental studies of the charge transport process in OTFTs show carriers conduct primarily through the first 1–5 ML above the gate dielectric.[8] Due to the presence of a large trap density, trap states dominate the carrier transport properties of organic films.[9] We hypothesize that analytes adsorbed on the surface of the CoPc films change both the doping level and the trap energy of the air/CoPc interface layer. The change in doping level affects the output current in both thin and thick channel devices. However, the changes in surface trap energy affect the charge transport more strongly in thin devices because the charge transport layers are closer to the air/CoPc interface as compared to the thick devices. The observed improvements in base line stability and dynamic response to gas sensing confirm the active participation of the surface traps in charge transport in the ultrathin transistors.

CoPc was purchased from Sigma-Aldrich and purified by zone sublimation below 10^{-5} Torr. Bottom-contact devices were fabricated on n^+ silicon wafers with 100 nm of thermally grown SiO_2. The channel length and width of the devices were 10 μm and 2 mm, respectively. CoPc thin films of 4 and 50 ML were deposited by OMBE at pressure of 2×10^{-9} Torr at 80 °C. Chemical sensing experiments were performed inside a custom built computer controlled flow system. Ultrathin OTFTs have been fabricated using high mobility but chemically nonspecific materials such as sexithiophene[10] and pentacene;[11] however, ChemFETs with thickness of a few monolayers have not been reported previously. Chemically selective materials, such as CoPc, generally have several orders of magnitude lower mobility than materials typically employed in the ultrathin OTFTs. Therefore, very careful control of the taper of the gold electrodes to avoid undercutting of the electrodes and three cycles of ultrasonication in trichloroethylene/acetone/isopropyl alcohol cleaning are required to ensure excellent contact between the CoPc channel films along the gold electrodes.

The devices were characterized in an optically isolated chamber at 25 °C. Each device was stabilized in a dry air flow for 3 days prior to chemical response measurements to equilibrate doping from atmospheric oxygen and humidity. Typical transfer curves are shown in Fig. 1(a). The mobility values extrapolated from the linear region are 1.0×10^{-4} and 2.6×10^{-4} $cm^2/V\,s$ for the 4 and 50 ML device. The lower mobility of the 4 ML device may be due to incomplete film coverage above the third layer or differences in film texture. Similarly, the mobility in pentacene films is reported to reach the bulk value only above 5 ML.[11] The threshold voltages extracted in the linear region by linearly extrapolating the transfer curves[12] [shown in Fig. 1(a)] between V_g (−4 to −10 V) are +0.38 and −0.38 V for the thin and thick devices. All the devices tested have been stored in a desiccator for 1 month and shown good reproducibility in chemical response from run to run and the chemical responses were

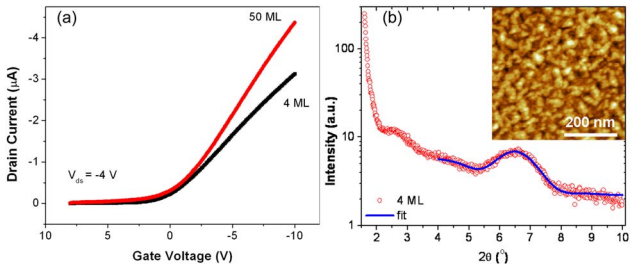

FIG. 1. (Color online) (a) Transfer characteristics of the 4 and 50 ML CoPc thin-film devices measured at $V_{ds}=-4$ V and V_g sweeps at 0.1 V/step at rate of 10 V/s. (b). X-ray diffraction for a 4 ML CoPc thin film grown on a SiO_2/Si substrate. The line is a fit using a quantitative refinement program. The inset shows the AFM image with a color scale range over 4.6 nm.

[a)]Electronic mail: akummel@ucsd.edu

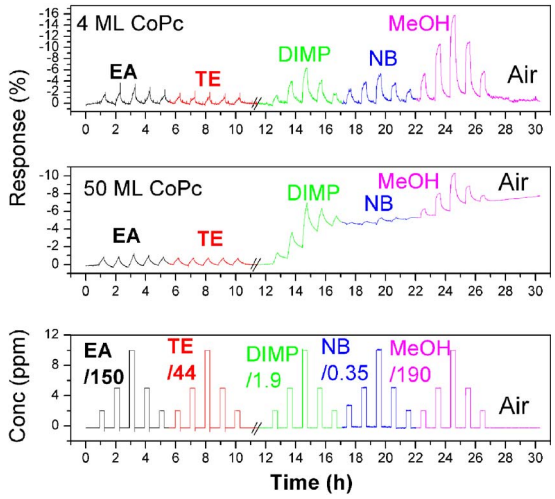

FIG. 2. (Color online) Chemical response to ethyl acetate (EA), toluene (TE), diisopropyl methylphosphonate (DIMP), nitrobenzene (NB), and methanol (MeOH) for 4 and 50 ML devices measured at V_{ds}=−4 V and V_g=−8 V. The broken lines represent two separate runs.

nearly independently of previous exposure to analytes. The aging procedure is required for the devices to achieve stable conductivity and chemical response. However, we note that the current noise is larger in the ultrathin ChemFET as compared to the thick ChemFET in aged devices. The noise level in the ultrathin devices was the same as the thick devices when they were less than 1 month old.

The nominal thickness determined by x-ray diffraction from a single CoPc thin film is 3.8 ML (51 Å) [see Fig. 1(b)]. The *d* spacing is 13.3 Å in accordance with previous measurements that show that the molecular planes of CoPc are oriented perpendicular to the substrate surface.[13] The surface morphology measured by atomic force microscopy (AFM) is shown in the inset of Fig. 1(b). The CoPc thin films grown at 80 °C have an average grain size of 36 nm and the surface rms roughness from AFM is 6.6 Å (for the bare substrate it is 0.9 Å). Since the average height from the AFM image amounts to only 2.3 nm, which is less than the nominal thickness, we infer that the CoPc film coverage is at least 2 ML everywhere on the film.

The devices were exposed to 25 chemical pulses; each exposure was 20 min long and followed by a 40 min recovery in a dry air flow. To minimize bias stress effect in devices by static gate bias,[14] a 0.1 Hz pulsed, 1% duty cycle gate bias was used for both devices. Note that the doses differ by two orders of magnitude between analytes so that the chemical response magnitudes appear to be similar for the different analytes (see Fig. 2). The chemical response is defined as $R \equiv (I_{\text{analyte}} - I_0)/I_0 100\%$, where I_0 is referred to the initial drain current.

The 4 ML device shows enhanced chemical response to all the analytes compared to the 50 ML device. The average enhancement factors ($R_{4\ \text{ML}}/R_{50\ \text{ML}}$), are between 1.5 and 20. The chemical responses here are calculated with a linearly extrapolated base line to account for the base line drift in each pulse. Any linear correlation between the enhanced chemical response and a molecular property, such as dipole moment or vapor pressure, is not readily apparent.

The chemical sensitivities of the thick and thin ChemFETs have been calculated by normalizing the chemical response by the analyte concentration. Since there are three different levels of analyte concentration (see Table I). Nonlinear chemical response and base line drift will contribute to the standard error in statistics. It is found that CoPc ChemFETs are over 200 more sensitive to NB as compared to the three organic volatile vapors (EA, toluene, and MeOH). Diluted NB concentrations as low as 75 ppb (ppb defined as parts per 10^9) were detected using the ultrathin device. This chemical sensitivity is among the best reported in the literature for nonredox active analytes on ChemFETs, but we note that far higher sensitivities have been obtained for highly oxidizing analytes (e.g., ozone) on NiPc ChemFETs.[15]

TABLE I. Average chemical sensitivity (S) in 10^{-3}%/ppm, drift (D) in %/h, and response time t_{50} in second of 4 and 50 ML devices to the vapor doses are extracted from Fig. 2. Note that the analytes are presented in order of sensitivity. The standard errors estimated from five pulses for each analyte are shown in parentheses. Drift below 0.05%/h is listed as nonsignificant (NS).

Analyte/Device		S(%)	D(%h)	$t_{50}(s)$
NB	4 ML	2372(345)	NS	134(14)
	50 ML	116(13)	0.07(0.04)	552(40)
DIMP	4 ML	400 (30)	0.26(0.05)	265 (30)
	50 ML	260 (10)	1.0 (0.1)	568 (42)
MeOH	4 ML	11 (1)	0.15 (0.15)	61 (14)
	50 ML	2.0 (0.2)	0.42 (0.05)	73 (16)
TE	4 ML	7.7 (2.2)	NS	420 (56)
	50 ML	5.4 (1.4)	NS	467 (17)
EA	4 ML	3.5 (0.7)	NS	558 (45)
	50 ML	2.0 (0.5)	NS	579 (15)

All five analytes reduce the drain current in both thin and thick films as a result of lower concentration of free carriers. This loss of free carriers can be ascribed to a reduced "surface doping" concentration, an increased trap energy, or both. The conductivity of CoPc films is very small in vacuum due to its low bulk doping.[16] Upon exposure to air, CoPc films conduct due to O_2 chemisorption at CoPc surface sites.[17] The conductivity gain through O_2 chemisorption at the air/CoPc interface is effectively equivalent to surface doping. For both thin and thick films, exposure to analytes changes the surface doping concentration, but we hypothesize that analytes can also change the trap energies involved in carrier transport in the ultrathin devices. The hypothesis that O_2 dopes the films and analytes creates a response as counterdopants is documented by comparing the sensor responses in air and N_2 carrier gases; these data show that the absolute responses in N_2 carrier gas are not only smaller than in air but also have a drift towards lower current.[18]

To simplify the quantification of the analyte induced changes in mobility, we operate the device at a gate voltage (−8 V) that is 20 times larger than V_t (−0.38 V and 0.38 V) in the linear region. Therefore, the chemical response is mainly determined by the change in mobility at a fixed V_g, $R = \Delta I/I_{\text{base}} = \Delta\mu/\mu_{\text{base}}$, where $\Delta\mu = \mu_{\text{analyte}} - \mu_{\text{base}}$. The effective mobility is related to trap energy E_a as $\mu = \mu_0 \exp(-E_a/kT)$, where μ_0 is the mobility related to the dopant concentration. We note that OTFT conductivities are modeled as a trap mediated conductivity so the carrier density does not appear explicitly in the equation and instead is incorporated into the mobility term.[8] In OTFTs, the charge carriers are transported in a few monolayers adjacent to the gate oxide;[8] therefore, the relevant trap energy E_a comes

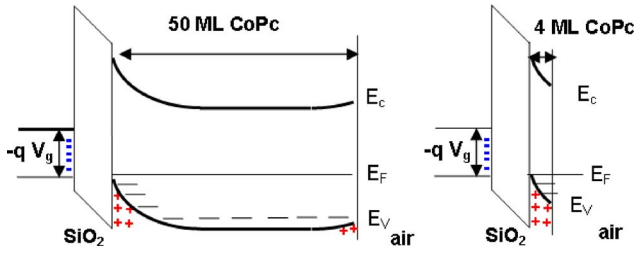

FIG. 3. (Color online) Electronic band models of thick and thin ChemFETs with a negative gate bias. Holes accumulate at the CoPc/SiO_2 interface by gate biasing and at the air/CoPc interface by oxygen doping. The broken lines represent trap states in the organic film.

from the CoPc/SiO_2 interface. Consequently, in thick films, the effect of the analyte on the relevant E_a is minimal because the analytes affect only the trap energies far from the CoPc/SiO_2 interface. Conversely, in ultrathin films, the air/CoPc surface is near the CoPc/SiO_2 interface so that the surface trap states affect the charge transport even at very high gate voltage. We note that the greatest enhancement for the response was observed for nitrobenzene, which should be a good hole trap since it has the largest dipole moment of the five analytes and probably the largest polarizability.

As shown in Fig. 2, the sensor base line drift over 20 h in the second run was reduced by a factor of 12 in the 4 ML device compared to the 50 ML device with pulsed gating. Base line drift has plagued OTFTs made from a wide range of materials.[14] With a static gate bias, the output current can diminish by 40% in 20 h. We found that a pulsed gate bias (0.5 Hz, 1% duty cycle) reduces the electrical drift in the absence of analytes in both 4 and 50 ML ChemFETs to 0.05%/h. The mean base line drift value is calculated for each analyte by measuring the accumulated drift each of the five pulses using the same starting point. For the analytes with significant drift (MeOH and DIMP), the base line drift is three to four times less in the ultrathin versus the thick ChemFETs. The overall drift difference over 20 h is larger because it takes account the cumulative drift of each chemical pulse. The reduced base line drift in the presence of analytes in ultrathin films may be attributed to the close location of the surface trap states to the gate dielectric. In ultrathin devices, the potential gradient from the gate is sufficiently strong and close to the oxide/CoPc interface that it tends to remove positive charges from the surface trap states, thereby reducing irreversible trapping that produces base line drift.

We have also observed faster dynamic response in ultrathin sensors, as shown in Table I. The turn-on response t_{50} is quantified by the time it takes to reach 50% of the maximum chemical response. While the response times for EA, toluene, and MeOH decrease by only 10%, for the other two analytes, the response time t_{50} is reduced by a factor of 2 in the 4 ML devices compared to the 50 ML devices. Generally, the t_{50} response time depends on the dose. The larger dose results in a faster response time for adsorption. For NB, the faster response time could be due to the increased sensitivity for ultrathin compared to thick ChemFETs. However, for DIMP, the improvement in response time is greater than the improvement in sensitivity for thin versus thick ChemFETs consistent with the electronic gas adsorption on semiconductor surfaces correlating with the film's Fermi level.[19]

To explain the effect of film thickness on ChemFET sensing, a qualitative electronic band diagram model illustrating the difference between the 4 and 50 ML devices is shown in Fig. 3. Positive holes are accumulated at the CoPc/SiO_2 interface by the gate capacitor and at the air/CoPc interface by oxygen surface doping. For ultrathin ChemFETs, the hole accumulation extends to the air/CoPc interface; therefore, the surface traps participate in carrier transport and the perturbation of the surface trap energies by the analytes renders the ultrathin ChemFETs more sensitive than the thick ChemFETs. The extension of the hole accumulation to the surface of the ultrathin ChemFETs is also responsible for the surface traps being depleted by the gate thereby reducing base line drift and changing the analyte absorption energy/kinetics.[19]

In conclusion, ultrathin ChemFETs have been reproducibly prepared by OMBE deposition. Due to the proximity of the air/CoPc interface to the charge transport layer in ultrathin ChemFETs, chemical response enhancements by a factor of up to 20 compared to thick ChemFETs have been observed. The effect can be ascribed to the analyte influencing not only just the surface doping but also the trap energy for carrier transport in ultrathin devices.

Funding from AFOSR MURI F49620-02-1-0288 and NSF CHE-0350571 was acknowledged.

[1] L. Torsi, A. Dodabalapur, L. Sabbatini, and P. G. Zambonin, Sens. Actuators B **67**, 312 (2000).
[2] B. Crone, A. Dodabalapur, A. Gelperin, L. Torsi, H. E. Katz, A. J. Lovinger, and Z. Bao, Appl. Phys. Lett. **78**, 2229 (2001).
[3] T. Someya, H. E. Katz, A. Gelperin, A. J. Lovinger, and A. Dodabalapur, Appl. Phys. Lett. **81**, 3079 (2002).
[4] Z. T. Zhu, J. T. Mason, R. Dieckmann, and G. G. Malliaras, Appl. Phys. Lett. **81**, 4643 (2002).
[5] L. Torsi and A. Dodabalapur, Anal. Chem. **77**, 380A (2005).
[6] J. B. Chang, V. Liu, V. Subramanian, K. Sivula, C. Luscombe, A. Murphy, J. S. Liu, and J. M. J. Frechet, J. Appl. Phys. **100**, 014506 (2006).
[7] M. Bouvet, Anal. Bioanal. Chem. **384**, 366 (2006).
[8] G. Horowitz, J. Mater. Res. **19**, 1946 (2004).
[9] R. Schmechel and H. von Seggern, Phys. Status Solidi A **201**, 1215 (2004).
[10] F. Dinelli, M. Murgia, P. Levy, M. Cavallini, F. Biscarini, and D. M. de Leeuw, Phys. Rev. Lett. **92**, 116802 (2004).
[11] R. Ruiz, A. Papadimitratos, A. C. Mayer, and G. G. Malliaras, Adv. Mater. (Weinheim, Ger.) **17**, 1795 (2005).
[12] D. K. Schroder, *Semiconductor Material and Device Characterization* (Wiley, New York, 1998), pp. 242-250.
[13] C. W. Miller, A. Sharoni, G. Liu, C. N. Colesniuc, B. Fruhberger, and I. K. Schuller, Phys. Rev. B **72**, 104113 (2005).
[14] J. B. Chang and V. Subramanian, Appl. Phys. Lett. **88**, 233513 (2006).
[15] M. Bouvet, G. Guillaud, A. Leroy, A. Maillard, S. Spirkovitch, and F. G. Tournilhac, Sens. Actuators B **73**, 63 (2001).
[16] A. W. Snow and W. R. Barger, *Phthalocyanines Properties and Applications* (Wiley, New York, 1989), Vol. 1, p. 345.
[17] J. D. Wright, Prog. Surf. Sci. **31**, 1 (1989).
[18] See EPAPS Document No. E-APPLAB-90-106724 for comparison of chemical responses in air and N_2. This document can be reached via a direct link in the online article's HTML reference section or via the EPAPS homepage (http://www.aip.org/pubservs/epaps.html).
[19] T. Wolkenstein, *Electronic Processes on Semiconductor Surfaces During Chemisorption* (Plenum, New York, 1991), pp. 1-100.